The Journal of Engineering

IET Journals
The Institution of Engineering and Technology

Modified hill climbing MPPT algorithm with reduced steady-state oscillation and improved tracking efficiency

eISSN 2051-3305
Received on 15th August 2018
Accepted on 31st August 2018
E-First on 5th November 2018
doi: 10.1049/joe.2018.8337
www.ietdl.org

Weiwei Zhu[1], Liqun Shang[1] ✉, Pengwei Li[1], Hangchen Guo[1]

[1]*College of Electrical and Control Engineering, Xi'an University of Science and Technology, Xi'an 710054, People's Republic of China*

✉ *E-mail: shanglq@xust.edu.cn*

Abstract: To ensure the photovoltaic (PV) system can still output maximum power under changing environmental conditions, a modified hill climbing algorithm is proposed. The algorithm uses a variable step-size strategy to reduce the steady-state oscillations and prevent operating point from diverging away from the maximum power point by introducing boundary conditions. To verify its effectiveness, the proposed algorithm is compared with the conventional and adaptive hill climbing method under the environmental condition of irradiance step change and gradual change. The simulation results show that the proposed algorithm can increase the dynamic response speed of the PV system by 75% under varying irradiance, and can achieve a steady-state tracking accuracy of 99.8%. Besides, the proposed algorithm only needs to embed several lines of additional programs in the conventional hill climbing maximum power point tracking (MPPT) control program and does not require additional hardware components, which reduces the cost of PV power generation.

1 Introduction

With the deterioration of the environment and the depletion of conventional energy sources, solar energy as a new type of green energy has attracted widespread attention throughout the world [1]. Photovoltaic (PV) array output current and output voltage are affected by meteorological conditions (irradiance, temperature etc.) and thereby appear to be non-linear. Its output power also changes continuously. Therefore, how to adjust the load characteristics so that the system can output the maximum power in real time as much as possible, namely, to achieve the maximum power point tracking (MPPT), is particularly important in the PV system [2, 3].

The literature [4–7] introduces several different MPPT control methods and soft computing techniques. Traditional MPPT methods mainly include hill climbing [8], perturbation and observation [9, 10], and incremental conductance methods [11], while the soft computing technology MPPT control method includes fuzzy-logic method [12], artificial neural network [13], and particle swarm optimisation [14]. Although its effectiveness has been verified by experiments in most cases, its algorithm still has the disadvantages of high complexity and slow convergence speed, so it is less applied to the actual engineering. The hill climbing method is currently the most widely used direct control method. Since it directly controls the duty cycle, it does not need to adjust the Proportional Integral (PI) increment, which simplifies the MPPT control structure and has a good control effect under stable external environment. However, this algorithm needs to constantly apply perturbation to the duty cycle to determine the maximum power point (MPP), so it will inevitably cause output power oscillation. At the same time, when the external environment gradually changes, it may cause the operation point to deviate from the MPP and the system undergoes serious oscillations, resulting in a lot of power loss. Xiao and Dunford [15] proposed an adaptive hill climbing method to solve the problems of power oscillation and slow response speed. Although this method can well take into account the dynamic and steady-state performances of the system, in the case of rapid change in irradiance, the adaptive mechanism may cause multiple errors in the tracking direction of the MPP, resulting in a large amount of power loss.

To maintain the fast response speed and high steady-state accuracy of the PV system under changing environmental conditions, this paper proposes a modified hill climbing algorithm. The algorithm mainly includes the following two characteristics: (i) a dynamic inspection mechanism, which can adjust the size of the perturbation step in real time according to the change of external irradiance; and (ii) establishing the duty cycle boundary to effectively avoid the deviation of the operating point from the MPP. Finally, a PV system simulation model is established in MATLAB to verify the effectiveness of the proposed algorithm.

2 PV array characteristic

Considering the economy and maintainability, a centralised inverter topology is generally used in PV power generation system. Centralised inverters are connected to a large number of PV modules, usually using S-P configuration. The generalised S-P structure model of the PV array is shown in Fig. 1. The output current equation of this topology can be expressed as follows [16]:

$$I = N_{\mathrm{pp}}\left[I_{\mathrm{pv}} - I_0(I_{\mathrm{p}} - 2)\right] - \left(\frac{V + IR_{\mathrm{s}}\Gamma}{R_{\mathrm{p}}\Gamma}\right) \tag{1}$$

where

$$I_{\mathrm{p}} = \exp\left(\frac{V + IR_{\mathrm{s}}\Gamma}{V_{\mathrm{T}}N_{\mathrm{ss}}}\right) + \exp\left(\frac{V + IR_{\mathrm{s}}\Gamma}{(p-1)V_{\mathrm{T}}N_{\mathrm{ss}}}\right) \tag{2}$$

$$\Gamma = \frac{N_{\mathrm{ss}}}{N_{\mathrm{pp}}} \tag{3}$$

where I is the solar cell output current, V is the solar cell work voltage, I_{pv} is the photocurrent, I_0 is the reverse saturation current, V_{T} is the thermal voltage of PV arrays, q is the electron charge $\left(1.60217 \times 10^{-19}\,\mathrm{C}\right)$, k is Boltzmann's constant $\left(1.38065 \times 10^{-23}\,\mathrm{J/K}\right)$, R_{s} is the equalised series resistance, R_{p} is the equalised parallel resistance, and N_{ss} and N_{pp} are the series and parallel PV arrays, respectively.

Fig. 2 shows the output power, output current, and output voltage characteristic curves of PV array under fixed ambient conditions. As can be seen from the current–voltage curve, PV array within the A–B range had basic equal output current, which could be considered that the PV array output characteristic of the left side of MPP as the current source, and that the array output current remained unchanged.

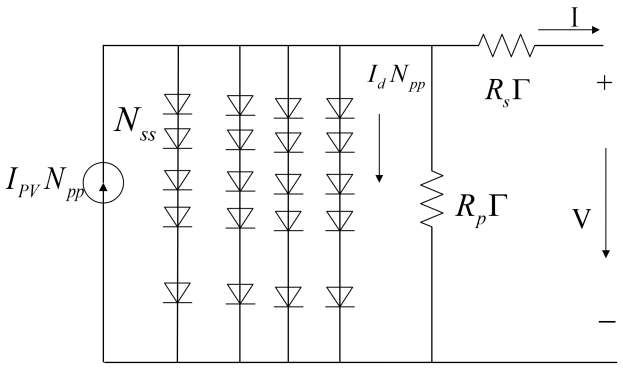

Fig. 1 *Equivalent circuit of S-P configuration of PV array*

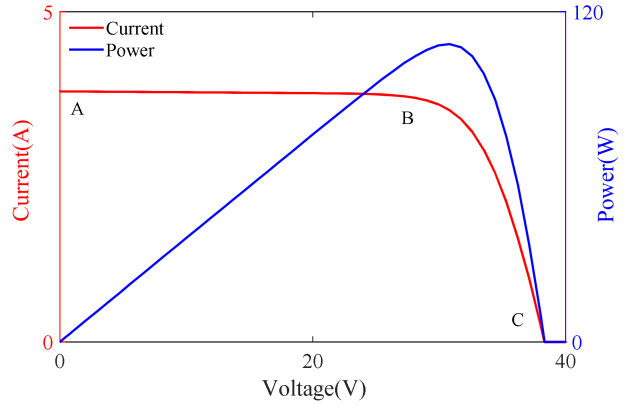

Fig. 2 *PV array characteristics under fixed ambient conditions*

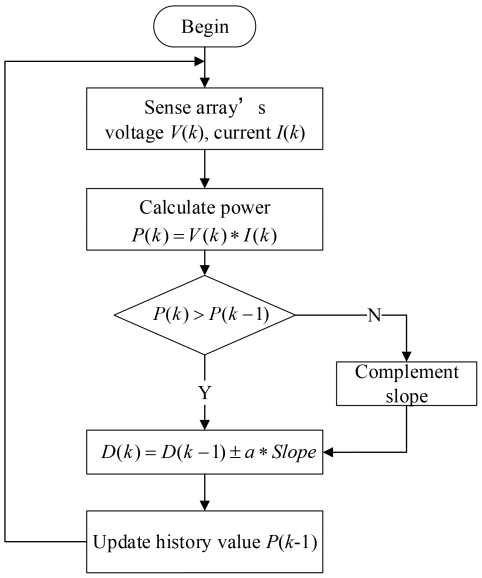

Fig. 3 *Flowchart for conventional hill climbing*

3 Proposed hill climbing algorithm

3.1 Conventional hill climbing

The most widely used MPPT algorithm is the hill climbing method, which generates a power change by applying a certain perturbation and confirms the controller's next action by detecting this change. The perturbation is the duty cycle. If the power is increased after the perturbation is applied, the control perturbation changes in the original direction with the power continuing to increase; when the power decreases, the perturbation is controlled in the opposite direction until the power change is within the set threshold. The perturbation step-size update rule is

$$D(k) = D(k-1) \pm a \times \text{Slope} \tag{4}$$

where $D(k)$ is the duty cycle, 'Slope' is a program variable, which indicates the direction that must follow on the P–D curve in order to increase the output power, and 'a' denotes the increment step size of duty cycle.

Fig. 3 shows the flowchart of the conventional hill climbing. Clearly, the step size of the perturbation 'a' is crucial; if 'a' is large, the convergence is fast, but it results in large fluctuation in output power and vice versa. Whatever may be the case, the conventional fixed-step hill climbing will result in operating point to continuously oscillate around the MPP, as depicted in Fig. 4.

3.2 Adaptive hill climbing

To solve the contradiction between the dynamic and steady-state performance of the conventional fixed-step hill climbing, the adaptive hill climbing introduces an adaptive mechanism based on the conventional method to intelligently change the size of the perturbation step to ensure the convergence of the method. When the operating point is far from the MPP, the perturbation step size is increased. As the operating point approaches the MPP, the perturbation step size is dynamically reduced until it attains a very small value.

There are various methods to change the perturbation step size. The duty cycle with variable step size can be given as follows [17]:

$$D(k) = D(k-1) \pm N\left(\frac{\mathrm{d}P}{\mathrm{d}V}\right) \tag{5}$$

where $\mathrm{d}P$ and $\mathrm{d}V$ are the derivatives of output power and voltage, respectively, while N is a constant parameter that requires tuning.

Although the adaptive hill climbing can solve the contradiction between the response speed and the steady-state accuracy of the conventional hill climbing, the adaptive mechanism may lead the operating point to deviate from the MPP locus when the irradiance changes gradually. As illustrated in Fig. 5, assume initially that the conventional hill climbing tracks the MPP at point A, and then the operating point vibrates among points A, B′, and B. When the operating point B moves to point A, the irradiance increases gradually, in which case the operating point might move towards point C′ rather than point B. If the MPPT judged that the current disturbance caused an increase in output power, the operating point would continue to disturb in the same direction, as shown in Fig. 5*a*. The operating point would move following the path of A–C′–D′–E′–F′, it could be clearly seen that the operating point has deviated from the MPP at the left of the P–V curve. For another situation, when the operating point moves from point B′ to point A, the irradiance increases gradually along with the increase in disturbance, the power increased, and the operating point would move to the right side of the P–V curve following the path of A–C–D–E–F and deviate from the MPP, causing a lot of power loss, as shown in Fig. 5*b*. However, it is worth noting that this phenomenon only occurred when the irradiance increased gradually, and it would never occur when the irradiance decreased gradually [18].

3.3 Proposed algorithm

The proposed algorithm is designed to enhance the performance of the conventional hill climbing by reducing the steady-state oscillation and preventing the divergence of the adaptive hill climbing from the MPP locus. Similar to other hill climbing, the proposed algorithm is based on the P–V characteristic curve of the PV array and the MPP is tracked by judging the differential sign of power versus voltage. When the operating D_{MPP} reaches the vicinity of the MPP, the perturbation step size is reduced to a minimum value by the variable step-size strategy. Due to the circuit noise and slight deviation of the irradiance and temperature, the tiny flickers can be handled by a small tolerance.

3.3.1 Variable step-size strategy: When the operating point reached the MPP, the disturbance step size had reached a certain minimum value, and then the power change rate ($\Delta P/P$) must be lower than a certain threshold value Γ_1. If $\Delta P/P > \Gamma_1$, it indicates the irradiance has changed (increased or decreased). In the actual

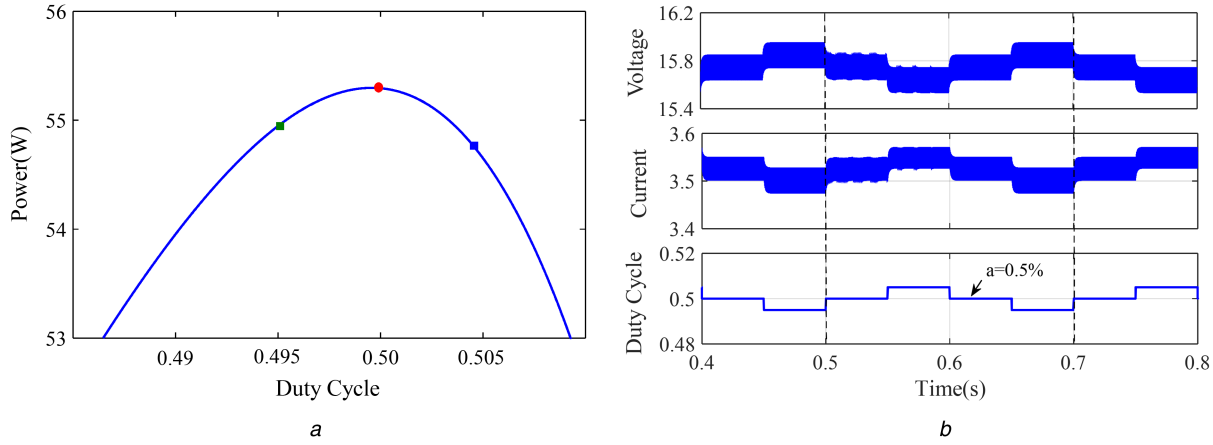

Fig. 4 *Simulations with $a = 0.5\%$, $T_a = 0.05$, and $S = 1000\ W/m^2$*
(a) Operating point location on PV characteristic, ***(b)*** Time-domain waveform

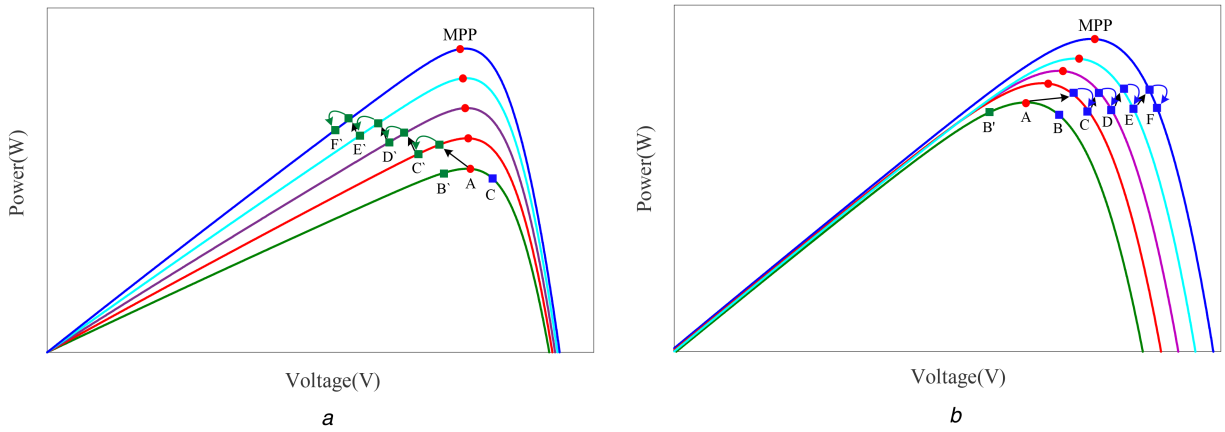

Fig. 5 *Loss of the tracking direction by adaptive hill climbing*
(a) Operating point towards the left side of MPP, ***(b)*** Operating point towards the right side of MPP

Table 1 Determination of the δ values

Symbol of dP	Symbol of dV	δ value
positive	positive	+1
positive	negative	−1
negative	positive	−1
negative	negative	+1

environment, the irradiance was changed in the following three ways: (i) slow change (1–10 W/m^2/s), (ii) fast change (>10 W/m^2/s), and step change. In order to determine whether the irradiance change was gradual or step, a threshold value Γ_2 was introduced in this paper. If $\Gamma_1 < \Delta P/P < \Gamma_2$, the system determined that the irradiance change was gradual, and in this case the disturbance step size increased gradually, which might also make the operating point to deviate from the MPP. To avoid this situation, it was necessary to set the duty cycle boundary and restrict the operating point D_{MPP} within the region of the MPP. Finally, when the irradiance change had stopped, the system detected the power change rate $\Delta P/P < \Gamma_1$ again, and the disturbance step size again decreased to the minimum value. If $\Delta P/P > \Gamma_2$, the system judged that the irradiance showed a step change, and the disturbance step size increased rapidly to ensure that the MPP could be rapidly tracked under the new irradiance.

3.3.2 Detection of steady-state oscillation: This paper uses dP and dV to determine the symbol of the perturbation direction in the value of δ, as shown in Table 1. The detection of steady-state oscillation is done by recording three consecutive values of δ. When the perturbation step size is decreasing, the symbol of δ is negative, and vice versa. During the decrease or increase in the perturbation step size, the three consecutive values of δ will be either positive or negative. Therefore, the absolute value of the summation of the δ value will be 3. After reaching the MPP, the steady-state oscillation begins; the operating point will move two times in one direction and then move to another direction. Thus, under successive oscillations, three consecutive symbols of δ will never be identical. These will be a combination of positive and negative. Thus, the absolute value of the summation of the δ value will always be <3. The algorithm detects steady-state oscillation by recording three consecutive values of δ. The following (6) is applied for the detection of steady-state oscillation [19]:

$$\text{if } \sum \text{symbol} = \begin{cases} 3 & \text{MPP converges to a steady state} \\ < 3 & \text{MPP will not converge to a steady state} \end{cases} \tag{6}$$

Equation (6) can be used to determine whether the operating point converges to the MPP. When the operating point converges to MPP, the variable step-size scheme is activated and the perturbation step size decreases until 0.005. Since it is small enough, the steady-state power loss is negligible.

3.3.3 Setting the duty cycle boundary condition: The proposed algorithm can decrease the perturbation step size after the convergence of the operating point to the MPP, thus it can deal with the gradual variation of the irradiance. However, the tracking direction is likely to be lost when the irradiance changes rapidly. To avoid this situation, a sign flag is introduced. Flag = 0 at the beginning, but once it detects $\Gamma_1 < \Delta P/P < \Gamma_2$, the system switches to flag = 1 and imposes a duty cycle boundary condition. The initial setting of the duty cycle boundary is [0.05, 0.95]. When the MPPT

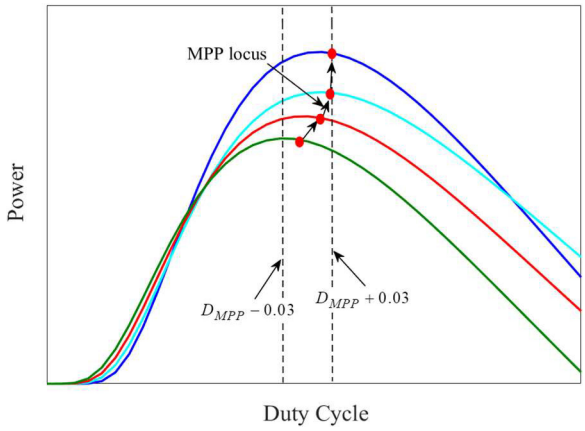

Fig. 6 *Restricting operating point near D_{MPP}*

Table 2 Parameters of the MSX-60 PV model at STC

Parameters	Variable	Value
short-circuit current	I_{sc}	3.8 A
open-circuit voltage	V_{oc}	21.1 V
current of P_{max}	I_{MPP}	3.5 A
voltage of P_{max}	V_{MPP}	17.1 V
maximum power	P_{MPP}	60 W
V_{oc} coefficient of temperature	K_v	−0.08 V/°C
I_{sc} coefficient of temperature	K_i	0.003 A/°C
no. of modules in series (per string)	N_s	36

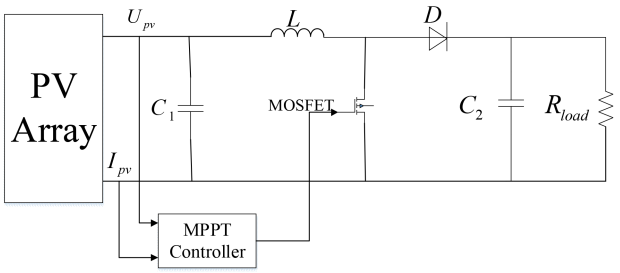

Fig. 7 *PV system with the boost converter*

detects flag = 1 (which means the oscillation has occurred), the boundary condition becomes $[D_{MPP}-0.03,\ D_{MPP}+0.03]$. This boundary condition is selected because when the irradiance gradually changes, D_{MPP} will also move slightly to the left or right. By setting the boundary conditions, the operating can be forced to stay near the MPP locus under conditions of gradation of the irradiance to avoid deviation from the tracking direction, as shown in Fig. 6.

Under the actual environment, the maximum change of irradiance was 27 W/m^2/s, and the maximum value of the power change rate could be 0.027 [20]. To ensure the effectiveness of the proposed method, the values of Γ_1 and Γ_2 were set to be 0.001 and 0.05, respectively. Therefore, when the irradiance changed between 1 and 50 W/m^2/s, the irradiance was considered to be gradual. When the irradiance change was greater than 50 W/m^2/s, it was considered as a step change.

4 Simulation results and analysis

This paper systematically simulates using the MATLAB 2017a software platform and uses Solarex-MX60 data of PV module customised by BP Solar for modelling. The parameters under standard test conditions (STC) are presented in Table 2. The simulation model for the converter of the PV system with the proposed MPPT algorithm is shown in Fig. 7. The following specifications for the boost converter are used: $C_1 = 470\,\mu$F, $C_2 = 47\,\mu$F, $L = 0.1$ mH, switching frequency = 10 kHz, and load resistance = 78 Ω. Furthermore, to ensure the system has attained a steady state before another MPP cycle is initiated, the sampling time is chosen to be 0.05 s.

4.1 Irradiance step-change simulation

The irradiance is set to leap from 400 to 1000 W/m^2 in 5 s, and suddenly drop to 400 W/m^2 in 10 s. Under the same conditions, we compare the performances of the conventional hill climbing, the adaptive hill climbing, and the proposed algorithm. The duty cycle and output power waveforms of each algorithm are shown in Fig. 8, and the simulation results are shown in Table 3.

Fig. 8*a* shows the simulation waveform of the conventional hill climbing with a perturbation step size of 0.01, and Fig. 8*b* shows the simulation waveform of the adaptive hill climbing. Comparing Figs. 8*a* and *b*, it can be seen that the system response times are 1.65 and 0.9 s when the irradiance suddenly increases from 400 to 1000 W/m^2 respectively. When the irradiance is 1000 W/m^2, the average output powers of the PV array are 107.6 and 109.7 W. When the irradiance suddenly decreases from 1000 to 400 W/m^2, the system response times are 1.6 and 2.5 s respectively. There is a faster response speed and a higher steady-state accuracy, but when the irradiance decreases, the adaptive hill climbing may fail, resulting in more power loss and reducing the system output efficiency.

Fig. 8*c* shows the simulated waveform of the modified hill climbing algorithm. Compared to the adaptive hill climbing method, when the irradiance suddenly rises from 400 to 1000 W/m^2, the system response time is decreased from the previous 0.9 to 0.4 s, which can reduce the response time by 1.9 s after the sudden decrease in the irradiance from 1000 to 400 W/m^2. At the same time, it can be seen from the duty cycle waveform diagram of the converter that the proposed algorithm has a small fluctuation in the duty cycle in the steady state and therefore the output power loss also remains small. When the irradiance is 400 W/m^2, the average output power of the proposed algorithm is 43.38 W, and the average output power of the 1000 W/m^2 irradiance is 111.05 W. Compared to the conventional hill climbing, the proposed algorithm can improve the steady-state tracking accuracy of MPPT from the previous 96.5 to 99.5%.

4.2 Irradiance gradual change simulation

The irradiance is set to start from 500 W/m^2 and increases from 500 to 580 W/m^2 during the slow gradual change (4–14 s). After being stabilised for 3 s, it rises from 580 to 800 W/m^2 during the fast gradual change (17–27 s), as shown in Fig. 9.

Under the same simulation conditions, the performances of the conventional hill climbing, the adaptive hill climbing, and the proposed algorithm are compared. The simulation waveforms of each algorithm are shown in Fig. 10.

Comparing Figs. 10*a* and *b*, it can be seen that at the beginning of the method, the system start-up times are 1.35 and 0.9 s, respectively, when the irradiance suddenly jumps from 0 to 500 W/m^2; when the irradiance is 500 W/m^2, the average output powers of the PV arrays are 52.6 and 54.3 W, respectively. It is indicated that the adaptive hill climbing can effectively increase the start-up speed, and the steady-state converter has less duty cycle oscillation and less output power loss. However, during the slow (4–14 s) and fast changes (17–27 s) in irradiance, the operating point of the adaptive hill climbing deviates from the tracking trajectory several times, and the duty cycle oscillates more severely, resulting in more power loss and the reduction in the output efficiency of the system.

Fig. 10*c* shows the simulated waveform of the proposed algorithm. Compared to the adaptive hill climbing method, the proposed algorithm reduces the system start-up time from previous 0.9 to 0.65 s. During the gradual change in the irradiance curve, it can be seen that the proposed algorithm almost perfectly tracks the irradiance curve and avoids the deviation of the operating point

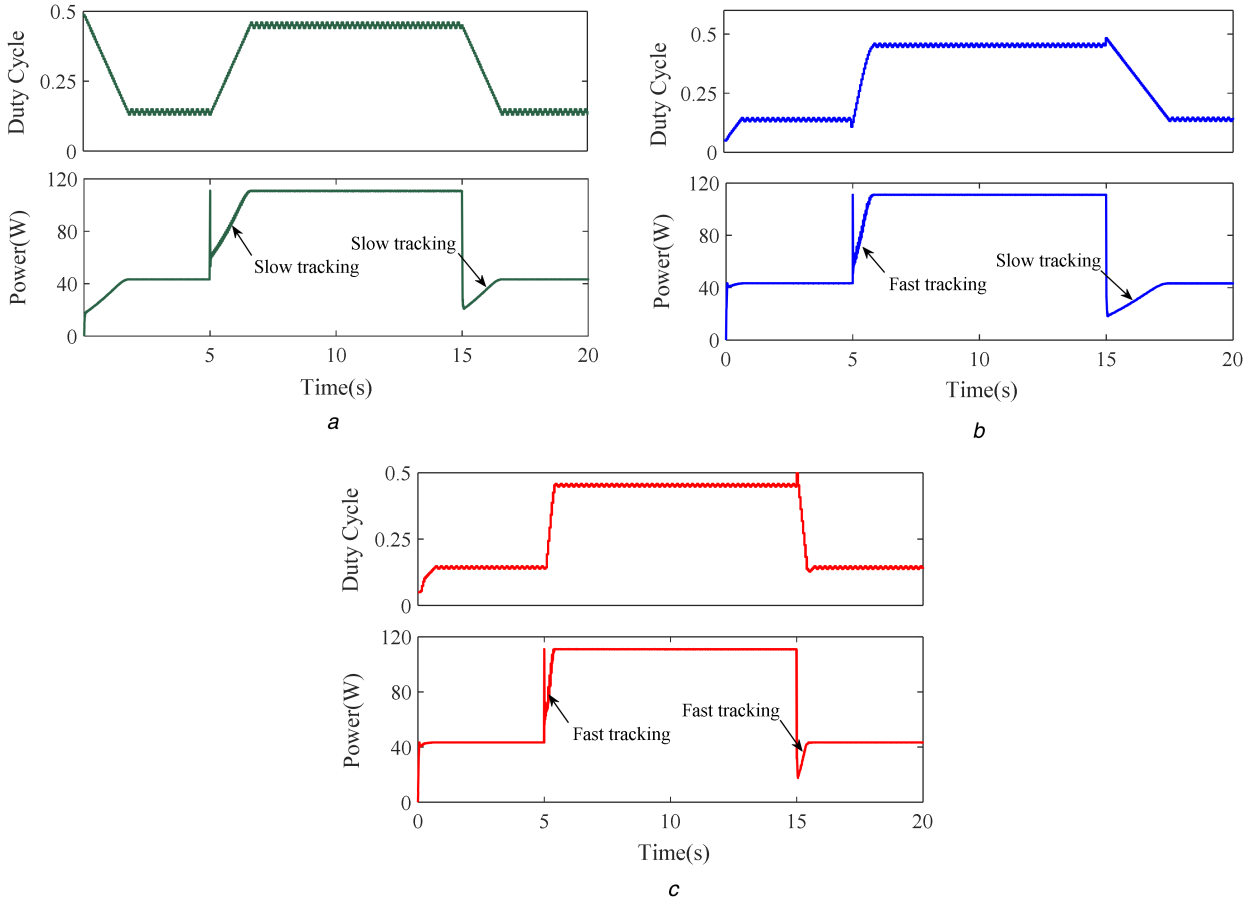

Fig. 8 *Tracking duty cycle and output power of different methods under the irradiance step change*
(a) Conventional hill climbing, ***(b)*** Adaptive hill climbing, ***(c)*** Proposed algorithm

Table 3 Comparison of simulation results

MPPT	Response time, s			Tracking accuracy at 1000 W/m^2, %	Tracking accuracy at 400 W/m^2, %
	Start-up	Irradiance increase	Irradiance decrease		
conventional hill climbing	1.9	1.65	1.65	96.5	96.7
adaptive hill climbing	1.0	0.9	2.5	98.3	98.6
proposed algorithm	0.65	0.4	0.6	99.5	99.8

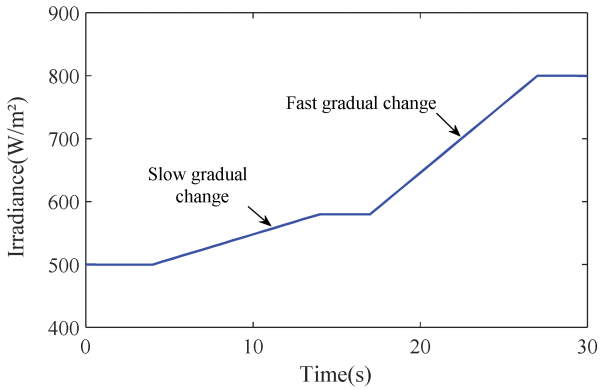

Fig. 9 *Irradiance profile for the change test*

from the MPP. At the same time, the duty cycle oscillates less, effectively improving the output efficiency of the PV array.

5 Conclusion

For the conventional hill climbing, the steady-state accuracy and dynamic tracking speed are difficult to take into account because of the step-size selection. The adaptive hill climbing method is easy to deviate from MPP locus under the conditions of gradual change in irradiance. This paper proposes a modified hill climbing algorithm and obtains the following conclusions through MATLAB/Simulink simulation:

(i) Under the step-change irradiance environment, the proposed algorithm can increase the system response speed by 75% as compared to the conventional hill climbing and can achieve the steady-state accuracy of 99.8%.
(ii) The proposed algorithm can solve the problem that the adaptive hill climbing deviates from the MPP locus while processing the irradiance gradation process, and effectively improves the output efficiency of the PV array.
(iii) Simulating the slow and rapid changes under real environment, the proposed algorithm has good steady-state and dynamic performances.

The proposed algorithm in this paper has a similar structure to the conventional method. In the actual application process, no additional hardware components are needed, which can be easily implemented using a low-cost microcontroller. Therefore, there is a maximum likelihood that this application can be used in the PV power generation system.

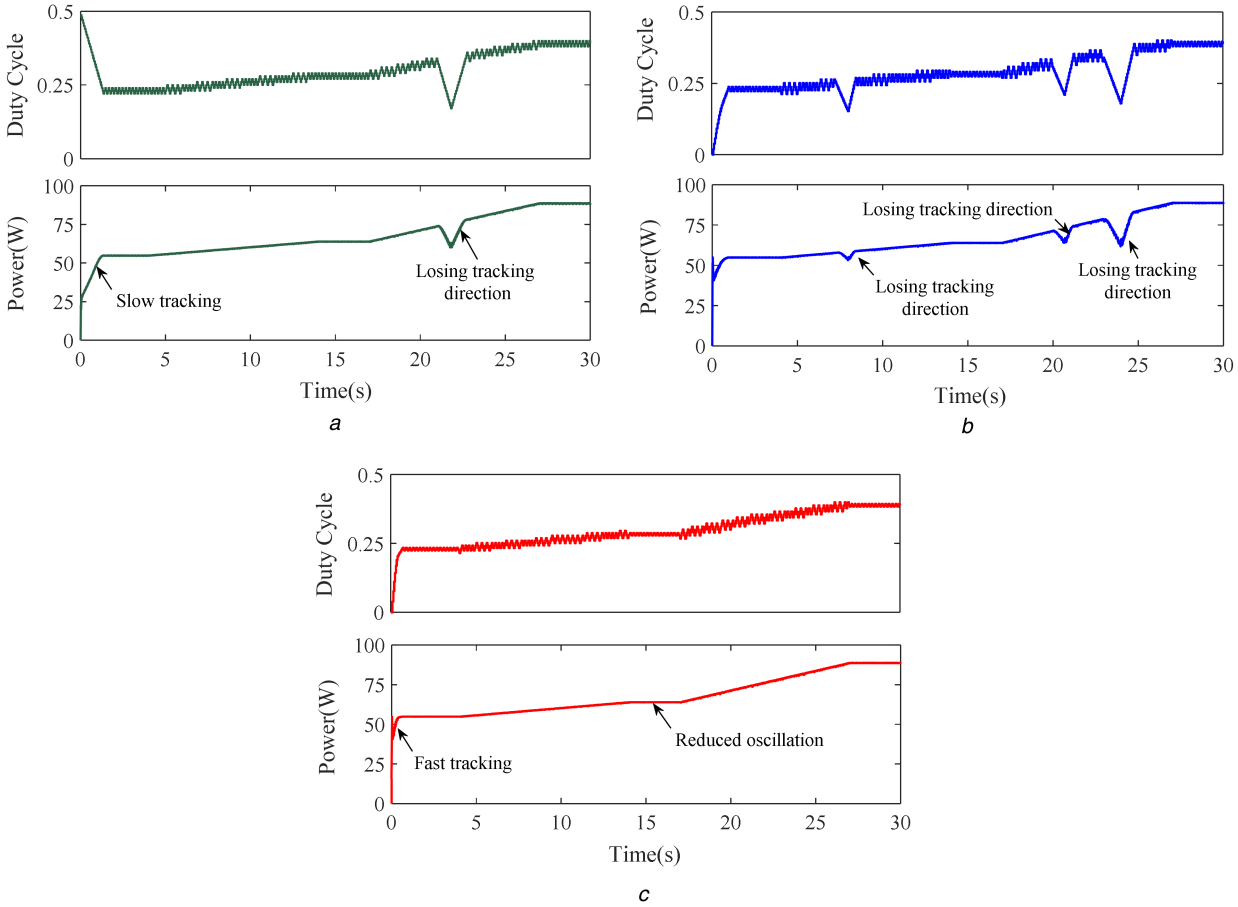

Fig. 10 *Tracking duty cycle and output power of different methods under the irradiance gradual change*
(a) Conventional hill climbing, ***(b)*** Adaptive hill climbing, ***(c)*** Proposed algorithm

6 Acknowledgments

This work was supported by the Natural Science Basic Research Plan in Shaanxi Province of China (Program No. 2014JM2-5077).

7 References

[1] Ram, J.P., Badu, T.S., Rajasekar, N.: 'A comprehensive review on solar PV maximum power point tracking techniques', *Renew. Sust. Energy Rev.*, 2017, **67**, pp. 826–848

[2] Wei, H., Liu, J., Yang, B.: 'Cost-benefit comparison between domestic solar water heater (DSHW) and building integrated photovoltaic (BIPV) systems for households in urban China', *Appl. Energy*, 2014, **126**, pp. 47–55

[3] Kadri, R., Gaubert, J.P., Champenios, G.: 'An improved maximum power point tracking for photovoltaic grid-connected inverter based on voltage-oriented control', *IEEE Trans. Ind. Electron.*, 2011, **58**, pp. 66–75

[4] Salam, Z., Ahmed, J., Merugu, B.S.: 'The application of soft computing methods for MPPT of PV system: a technique and status review', *Appl. Energy*, 2013, **107**, pp. 135–148

[5] Ahmed, J., Salam, Z.: 'A critical evaluation on maximum power point tracking methods for partial shading in PV systems', *Renew. Sust. Energy Rev.*, 2015, **47**, pp. 933–953

[6] Esram, T., Chapman, P.L.: 'Comparison of photovoltaic array maximum power point tracking techniques', *IEEE Trans. Energy Convers.*, 2007, **22**, pp. 439–449

[7] Alagmi, B.N., Ahmed, K.H., Finney, S.J., *et al.*: 'Fuzzy-logic-control approach of a modified hill-climbing method for maximum power point in microgrid standalone photovoltaic system', *IEEE Trans. Power Electron.*, 2011, **26**, pp. 1022–1030

[8] Kjar, S.B.: 'Evaluation of the hill climbing and the incremental conductance maximum power point trackers for photovoltaic power systems', *IEEE Trans. Energy Convers.*, 2012, **27**, pp. 922–929

[9] Femia, N., Petrone, G., Spagnuolo, G., *et al.*: 'Optimization of perturb and observe maximum power point tracking method', *IEEE Trans. Power Electron.*, 2005, **20**, pp. 963–973

[10] Dabra, V., Paliwal, K.K., Sharma, P., *et al.*: 'Optimization of photovoltaic power system: A comparative study', *Prot. Control Mod. Power Syst.*, 2017, **2**, pp. 29–39

[11] Tey, K.S., Mekhilef, S.: 'Modified incremental conductance MPPT algorithm to mitigate inaccurate responses under fast-changing solar irradiation level', *Sol. Energy*, 2014, **101**, pp. 333–342

[12] Khateb, A.E., Rahim, N.A., Selevaraj, J., *et al.*: 'Fuzzy-logic-controller-based sepic converter for maximum power point tracking', *IEEE Trans. Ind. Appl.*, 2014, **50**, pp. 2349–2358

[13] Boumaaraf, H., Talha, A., Bouhali, O.: 'A three-phase NPC grid-connected inverter for photovoltaic applications using neural network MPPT', *Renew. Sust. Energy Rev.*, 2015, **49**, pp. 1171–1179

[14] Ishaque, K., Salam, Z.: 'A deterministic particle swarm optimization maximum power point tracker for photovoltaic system under partial shading condition', *IEEE Trans. Ind. Electron.*, 2013, **60**, pp. 3195–3206

[15] Xiao, W., Dunford, W.: 'A modified adaptive hill climbing MPPT method for photovoltaic power systems'. Proc. 35th IEEE Power Electronics Spec. Conf., Aachen, Germany, June 2004, pp. 1957–1963

[16] Ishaque, K., Salam, Z., Taheri, H., *et al.*: 'Accurate MATLAB simulation PV system simulator based on a two-diode model', *J. Power Electron.*, 2011, **11**, pp. 179–187

[17] Liu, F.R., Duan, S., Liu, F., *et al.*: 'A variable step size INC MPPT method for PV system', *IEEE Trans. Ind. Electron.*, 2008, **55**, pp. 2622–2628

[18] Bannett, T., Zilouchian, A., Messenger, R.: 'A proposed maximum power point tracking algorithm based on a new testing standard', *Sol. Energy*, 2013, **89**, pp. 23–41

[19] Ahmed, J., Salam, Z.: 'A modified P&O maximum power point method with reduced steady-state oscillation and improve tracking efficiency', *IEEE Trans. Sust. Energy*, 2016, **7**, pp. 1506–1515

[20] Bletterie, B., Bruendlinger, R., Spielauer, S.: 'Quantifying dynamic MPPT performance under realistic conditions first test results – The way forward'. Proc. 21st Eur. Photovolt. sol. Energy Conf., Dresden, Germany, September 2006, pp. 1–7